



LAWRENCE
LIVERMORE
NATIONAL
LABORATORY

Assessment of thermo-electric techniques for scrape-off layer current drive in slab geometry

I. Joseph, T. D. Rognlien

May 26, 2010

Journal of Nuclear Materials

Disclaimer

This document was prepared as an account of work sponsored by an agency of the United States government. Neither the United States government nor Lawrence Livermore National Security, LLC, nor any of their employees makes any warranty, expressed or implied, or assumes any legal liability or responsibility for the accuracy, completeness, or usefulness of any information, apparatus, product, or process disclosed, or represents that its use would not infringe privately owned rights. Reference herein to any specific commercial product, process, or service by trade name, trademark, manufacturer, or otherwise does not necessarily constitute or imply its endorsement, recommendation, or favoring by the United States government or Lawrence Livermore National Security, LLC. The views and opinions of authors expressed herein do not necessarily state or reflect those of the United States government or Lawrence Livermore National Security, LLC, and shall not be used for advertising or product endorsement purposes.

**Assessment of thermo-electric techniques for
scrape-off layer current drive in flux-tube geometry**

I. Joseph and T. D. Rognlien

Lawrence Livermore National Laboratory, 7000 East Ave., Livermore, CA 94551, USA

Abstract

The magnitude of the parallel current that can be driven by asymmetries between divertor target plates is calculated in magnetic flux-tube geometry. Current can be driven between ends of the flux tube by passive techniques that generate a thermo-electric potential by heating or cooling one side relative to the other through pumping or neutral gas injection. The thermo-electric potential primarily depends on the total particle flux pumped relative to the total recycling flux, but, for the geometry considered, pumping efficiency is higher for pumping by the target plate or from the private flux zone than for pumping from the outer side of the plate. Neutral gas injection is not as effective at generating an asymmetry. An important constraint for these methods may be the additional heat flux delivered to the hotter target, but additional Ohmic heating is much smaller than that generated by electrical biasing.

PACS: 52.40.Hf, 52.40.Kh, 52.55.Fa, 52.55.Hc, 52.65.Kj

JNM keywords: Plasma-Materials Interaction, Plasma Properties, Theory and Modeling

PSI-16 keywords: Divertor asymmetry, ELM, Plasma sheath, SOL current, UEDGE

**Corresponding author address:* Fusion Energy Program L-630, Lawrence Livermore National Laboratory, 7000 East Ave., Livermore CA 94551, USA.

**Corresponding author E-mail:* joseph5@llnl.gov

1. Introduction

Control of the impulsive heat fluxes delivered by edge-localized modes (ELMs) is a critical requirement for acceptable divertor lifetimes for high-performance tokamak reactors. Toroidally asymmetric scrape-off layer (SOL) currents are predicted [1,2] to significantly affect the edge plasma pressure gradient and, thus, magneto-hydrodynamic stability if sufficient non-axisymmetric SOL current can be driven. Because the induced SOL current is primarily parallel to the equilibrium magnetic field, it generates a primarily perpendicular magnetic field perturbation that is highly resonant with the pitch of field lines near the separatrix [1,2]. This generates a naturally edge-localized resonant magnetic perturbation (RMP) spectrum [2,3]. RMPs have been shown to experimentally stabilize and de-stabilize edge localized modes by controlling edge plasma profiles [4-8]. The advantage of utilizing a technique that is not based on magnetic coils or electrical biasing is that it may avoid the complex engineering constraints that need to be applied to the design of insulators and current-carrying coils in a high magnetic field and high neutron-flux environment.

Demonstration that reactor-relevant current drive techniques can indeed generate the required level of SOL current is a crucial step. In this work, we perform a qualitative assessment of the ability of passive techniques that utilize toroidally localized pumping and gas injection to generate a toroidal asymmetry that drives SOL current from one target plate to the other. The toroidal phase of the current is constant along a flux tube (as in Fig. 1. of Ref. [1]), but alternate flux tubes have different conditions near the target plate that generate the toroidal asymmetry, e.g. differential pumping or different target plate materials. The full evaluation of these techniques will require a 3D calculation. However, since low toroidal mode numbers, $n=1-3$, have been previously identified as most promising, the relevant perturbations have slow toroidal variation. Here, the UEDGE code [8] is used to qualitatively evaluate these techniques by modeling the SOL plasma as a two-dimensional flux tube that winds around the device along

the direction of the magnetic field. The geometry of the flux tube is approximated as a slab with negligible toroidal variation and the study of toroidal effects is left to future work.

The sheath potential at the target plate can be altered with a variety of techniques such as heating by gas pumping or cooling by gas fueling or impurity radiation [9]. The divertor conditions are most sensitive when close to the transition to a highly radiative and/or attached plasma state [10]. For a single-null tokamak, there is usually a significant poloidal asymmetry between the inner and outer divertor targets due to the effects of toroidal geometry. Experiments and simulations show that the naturally driven current density in present tokamaks is of order $\sim 1-10 \text{ A/cm}^2$ [9,11-15], similar to the magnitude needed for ELM control. Thus, in practice, it should also be effective to attempt to locally balance a natural poloidal asymmetry at alternating toroidal locations rather than drive asymmetries.

The potential difference across the sheath, between the plasma and the wall, is given by

$$\Phi_{\text{plasma}} - \Phi_{\text{wall}} = \Phi_{\text{float}} + (T_e/e) \log(1 + \vec{J} \cdot \hat{n} / J_{\text{sat}} \hat{b} \cdot \hat{n}) \quad (1)$$

where J is the current density and \hat{n} is the unit normal from the wall into the plasma. Current densities as large as the ion saturation current density $J_{\text{sat}} = en_e c_s$, will be driven through the edge plasma if the sheath potential differs from the floating potential by $O(T_e/e)$. Here e is the electron charge, n_e is the electron density, T_e is the electron temperature, and c_s is the sound speed. The sheath is composed of both a capacitor (the first term Φ_{float}) and a nonlinear resistor (the second term). The floating potential $\Phi_{\text{float}} = \Lambda_{\text{sheath}} T_e/e$ is primarily determined by T_e in the sheath; the constant of proportionality $\Lambda_{\text{sheath}} = \frac{1}{2} \log(v_{te}^2 / 2\pi c_s^2)$ is in the range of 2-4 for plasma conditions in the simulations below, where the electron thermal velocity is $v_{te} = (T_e/m_e)^{1/2}$ with electron mass m_e . To lowest order, the potential difference between the two ends of a magnetic field line in the plasma is determined by parallel electron momentum balance

$$\Delta \Phi_{\text{plasma}} = \int dp_e / en_e + \Delta(\alpha T_e/e) - \int \eta_{\parallel} J d\ell \quad (2)$$

where p_e is the electron pressure, η_{\parallel} is the parallel resistivity and $\alpha=0.71$ for a collisional plasma. The total bias potential balances the total potential drop due to plasma and sheath resistance; it can be decomposed as $\Delta\Phi_{\text{bias}}=\Delta\Phi_{\text{thermo}}+\Delta\Phi_{\text{wall}}$, the sum of the thermo-electric potential and the wall potential difference maintained by the external circuit. Thus, the total thermo-electric bias potential $\Delta\Phi_{\text{thermo}}$ is defined to be

$$\Delta\Phi_{\text{thermo}} = \Delta\Phi_{\text{float}} - \int dp_e / n_e - \Delta(\alpha T_e / e). \quad (3)$$

If the capacitors in the two sheaths are not balanced, $\Delta\Phi_{\text{float}}$ acts as a simple battery to drive current from the hot end to the cold end. However, the T_e and p_e gradients typically oppose the floating potential; e.g., for the case of constant electron pressure, $\Delta\Phi_{\text{thermo}} = \Delta [(\Lambda_{\text{sheath}} - \alpha) T_e / e]$.

The RMP produced by the parallel SOL surface current density $I = \int j d\ell$ is of order $\delta B \sim \epsilon_{\text{SOL}} \mu_0 I / 2$ where ϵ_{SOL} is the efficiency with which the SOL current produces a coherent perturbation [1,2]. ELM control is experimentally observed [4-8] to occur at a threshold in RMP strength of order $\delta B / B > 10^{-4}$. In engineering units, this requires a minimum efficiency

$$\epsilon_{\text{SOL}} > B_T / 2\pi I_{\text{kA/m}}. \quad (4)$$

The efficiency can vary greatly depending on the toroidal mode number, the phasing at the target plate, and the radial distribution of current density in the SOL. Analytic estimates are summarized in Ref. 1 (c.f. Fig. 7) and show that at low toroidal mode number $\epsilon_{\text{SOL}} > 10\%$ can typically be achieved by moving the location of the strike point relative to the biasing region.

2. Computational Results

We use the UEDGE code [8] to model the plasma as a ‘‘flux-limited’’ Braginskii plasma with the addition of diffusive transport coefficients assumed to be generated by turbulence. The toroidal field is constant $B_z = 2\text{T}$ and is assumed to be 10 times larger than the poloidal field. The geometry represents a 30m long flux tube that winds 3m poloidally from one divertor plate to the other. The simulation domain is the slab shown in Fig. 1 with 17 radial \times 32 poloidal cells.

The model distinguishes a “core” region that is 2m long poloidally (16 cells) and two divertor legs that are each 0.5m long poloidally (8 cells). The SOL is 4.5cm thick (16 cells), but the core and private flux regions are only 0.05cm thick (1 cell). For simplicity, the transport model has a constant perpendicular particle diffusivity $D=0.333\text{m}^2/\text{s}$, perpendicular viscous diffusivity $\eta=1\text{m}^2/\text{s}$, toroidal momentum diffusivity $D_v=0.4\text{m}^2/\text{s}$, and radial thermal diffusivity $\chi=1\text{m}^2/\text{s}$ for all species. Charge exchange collisions between deuterium ions and neutrals are assumed to be rapid enough to equilibrate their temperatures.

We begin with a symmetric divertor configuration and then intentionally introduce an asymmetry that drives current towards the right plate. On the core boundary, the density and temperatures are assumed to be constant with $n_{i,\text{core}}=2\times 10^{19}\text{m}^{-3}$. The core power injected into the flux tube is $P_i=P_e=0.1\text{MW}/\text{m}$ times the toroidal width of the tube; all fluxes are reported per unit toroidal width. For a tokamak with a toroidal circumference of 10m, the total injected power would be 2MW. The core density corresponds to typical separatrix densities achieved during ELM control experiments on DIII-D [4,5], but the injected power is low, only 1/5-1/2 of typical experimental injected powers. The boundary condition for total particle flux Γ lost to the plate is

$$\Gamma = (1 - R_i)n_i c_s + (1 - A_n)n_n v_n \quad (5)$$

where n_i is the ion density, n_n is the neutral density and $v_n=(T/2\pi m_n)^{1/2}$ is the neutral escape speed with mass m_n . The default configuration assumes an ion recycling coefficient $R_i=0.99$ (1% “wall pumping”) and a neutral albedo $A_n=1$ (no neutral pumping).

To quantify how any parameter X affects current drive over the entire target, the average of X weighted by the current density distribution on each target plate is defined via $\langle X \rangle = \int X J d\ell / I$. Local quantities are shown in Fig. 2 while average results are shown in Fig. 3 and summarized in Table 1.

Symmetric Solution: The solutions along the divertor target plates are shown in Fig. 2a. The target plate parameters peak at $T_e=5.5\text{eV}$, $n_i=5.5\times 10^{20}\text{m}^{-3}$ and $n_n=1.8\times 10^{20}\text{m}^{-3}$. The radiated

power fraction is 13% and the output power to each plate is $P_{\text{right}}=P_{\text{left}}=0.092\text{MW/m}$, including radiation. With these target conditions, J_{sat} peaks at 19A/cm^2 and, in principle, it is possible to drive $I_{\text{sat}}=22\text{kA/m}$ which only requires $\epsilon_{\text{SOL}}>1.4\%$.

Electrical Biasing: For comparison to the passive methods of interest, the bias potential $\Delta\Phi_{\text{wall}}$ is raised from 0 to 95V driving current from left to right. At 95V, I_{\parallel} (green) reaches 17kA/m or 82% of I_{sat} . Heating of the left side raises T_e to $\sim 20\text{eV}$, as seen in Fig. 2b. Figure 3a shows that a substantial thermal asymmetry $T_{e,\text{right}}/T_{e,\text{left}}$ (red) is induced and then saturates, providing an additional bias of $\Delta\Phi_{\text{thermo}}\sim 4\text{-}5\text{V}$ (black). There is also an additional 0.21MW/m of Ohmic heating power, of which 0.16MW/m must be supplied by the biasing system. The left plate now absorbs much of the power $P_{\text{left}}=0.37\text{MW/m}$ and the radiated power fraction drops to 8%.

Pumping: The results in Fig. 3b show that the ability of a given additional pumping flux to induce an asymmetry and drive a potential difference is relatively independent of the manner in which the pumping is performed. A significant asymmetry is generated when the total ion current pumped $I_{\text{pump}} = \int e\Gamma dl$ is a few percent of the total parallel ion saturation current $I_{\text{sat,tot}}=I_{\text{sat,left}}+I_{\text{sat,right}}$. For the symmetric case, the target plate boundary condition fixes $I_{\text{pump}}/I_{\text{sat,tot}}=1\%$. The essential difference between the techniques below lies in the pumping efficiency.

The ion-recycling coefficient R_i controls the amount of ‘‘wall pumping’’ for the target plate material. Using different materials, e.g. Li vs. C, for different sections of the target plate can be a useful means of driving current in a short pulse device. For a long pulse device, this asymmetry drive is expected to terminate once the walls become completely saturated with particles. The recycling scan in Fig. 3b shows that $I_{\parallel}=6.2\text{kA/m}$ can be driven for $R_i=85\%$ which is 56% of I_{sat} . ELM control requires $\epsilon_{\text{SOL}}>6\%$, comparable to direct biasing, but with no additional input power needed, only 0.04MW/m of Ohmic heating, and less power to the left plate $P_{\text{left}}=0.16\text{MW/m}$.

An equivalent technique is to pump neutrals near one of the targets. First, consider placing a pump on the inner edge of the left target plate, in the private flux zone. The pump covers half the length of the divertor leg, 0.25m poloidally, and removes incident neutrals with probability $1-A_n$, as described in Eq. 4. The results are shown in Figs. 2c and 3b (data marked with ‘o’). As the albedo reaches $A_n=85\%$, the pumping induced asymmetry can drive 4.9kA/m of current. In this case, there is 0.02MW/m of Ohmic heating and the power on the left plate is $P_{\text{left}}=0.18\text{MW/m}$. Next, consider a placing pump on the outer edge of the left target plate, in the outer SOL. The pump covers the entire length of the left divertor leg, 0.5m poloidally. Results shown in Fig. 3b (data marked with ‘x’) are close to the previous cases. In this case, 3.5kA/m of parallel current can be driven at $A_n=85\%$. This pump location does not couple to the strike point region as efficiently as the previous case and requires $\epsilon_{\text{SOL}}>9\%$. The efficiency should actually increase because a larger fraction of the saturation current is driven further from the strike point (see Fig. 2d). Ohmic heating is reduced to 8kW/m and the power to the left plate is now $P_{\text{left}}=0.15\text{MW/m}$.

Neutral Injection: An alternate technique for current drive is to cool the plasma by injecting neutral gas at the other plate. In this scan, neutrals are injected through a port 0.5m long on the outer/SOL side of the right plate. The current drive has a wide maximum occurring near a neutral injection current of $I_n = 70\text{A/m}$, but only 1.6kA/m of current can be driven, roughly 6% of the saturation current, which has increased due to the increase in ion density. ELM control would require $\epsilon_{\text{SOL}}>20\%$. One might seek to enhance the effect by injecting gas at one target plate and pumping at the other end. Consider the case of pumping with fixed $A_n=85\%$ and injecting neutrals, both in the outer SOL with the geometry above. The maximum effect is realized for a neutral injection current near $I_n=40\text{A/m}$, but the effect only generates a 12% enhancement over pumping alone, $I_{\parallel}=3.9\text{kA/m}$. While this could achieve enhanced toroidally symmetric current drive, in the toroidally asymmetric case it would be difficult to match the correct radial and toroidal phases between target plates near the strike point [1,2].

3. Discussion

For the current drive techniques considered above, the SOL current can exceed the ELM control threshold if $\epsilon_{\text{SOL}} > 5\text{-}20\%$. Because the ion saturation current increases strongly with input power, even less efficiency would be required at higher power. For the geometry considered, “wall pumping” and pumping from the private flux zone both efficiently couple to the strike point and can drive a significant fraction of the total saturation current. Although producing less total current, pumping and/or injecting neutral gas into the outer SOL generates current further from the strike point, which can increase the coherence efficiency. An important constraint for these methods may be the additional heat flux delivered to the hotter target, but additional Ohmic heating is much smaller than that generated by electrical biasing. These preliminary conclusions motivate further study in realistic 3D toroidal geometry that includes the interaction between toroidal and poloidal asymmetries which can affect the nonlinear saturation point. With optimization, passive current drive methods may have enough efficiency to control edge and SOL instabilities in a high-power tokamak.

Acknowledgements

The authors would like to thank R.H. Cohen, G.D. Porter, D.D. Ryutov, G.M. Staebler and M.V. Umansky for interesting discussions on the subject of current drive. This work was performed for U.S.D.O.E. by L.L.N.L. under Contract DE-AC52-07NA27344.

References

- [1] I. Joseph, R. H. Cohen and D. D. Ryutov, Phys. Plasmas **16** (2009) 052510.
- [2] I. Joseph, Phys. Plasmas **16** (2009) 052511.
- [3] I. Joseph, Contrib. Plasma Phys. **50** (2009) 317.
- [4] K. H. Burrell, T. E. Evans, E. J. Doyle, et al., Plasma Phys. Control. Fusion **B37** (2005) 47.

- [5] T. E. Evans, K. H. Burrell, M.E. Fenstermacher, et al., *Nature Phys.* **2** (2006) 419.
- [6] Y. Liang, H. R. Koslowski, P. R. Thomas, et al., *Phys. Rev. Lett.* **98** (2007) 265004.
- [7] J. Canik, R. Maingi, T. Evans, et al., *Proc. 22nd IAEA Fusion Energy Conference* (2008), paper PD/P1-5.
- [8] E. Nardon, A. Kirk, R. Akers, et al., *Plasma Phys. Control. Fusion* **51** (2009) 124010.
- [9] T. D. Rognlien, J. L. Milovich, M. E. Rensink and G. D. Porter, *J. Nucl. Mater.* **196-198** (1992) 347.
- [10] R. H. Cohen and D. D. Ryutov, *Phys. Plasmas* **2** (1995) 2011.
- [11] G. M. Staebler, *Nucl. Fusion* **36** (1996) 1437.
- [12] P. J. Harbour, *Contrib. Plasma Phys.* **28** (1988) 417.
- [13] P. J. Harbour, D. D. R. Summers, S. Clement, et al., *J. Nucl. Mater.* **162-164** (1988) 236.
- [14] A. V. Chankin, S. Clement, L. de Kock, et al., *J. Nucl. Mater.* **196-198** (1992) 739.
- [15] A. V. Chankin, *J. Nucl. Mater.* **241-243** (1997) 199.

Table Captions

Table 1. The average asymmetry and thermo-electric potential driven by various techniques determines the parallel current and the minimum efficiency required for $B=2T$ and $\delta B/B > 10^{-4}$.

Tables

Method	Parameter	$\left\langle \frac{n_{e,\text{left}}}{n_{e,\text{right}}} \right\rangle$ (%)	$\left\langle \frac{T_{e,\text{right}}}{T_{e,\text{left}}} \right\rangle$ (%)	$\langle \Phi_{\text{thermo}} \rangle$ (V)	I_{\parallel} (kA/m)	$I_{\text{sat},\text{right}}$ (kA/m)	$\frac{I_{\parallel}}{I_{\text{sat},\text{right}}}$ (%)	ϵ_{SOL} (%)
Electric Bias	$\Delta\Phi_{\text{wall}}=95\text{V}$	46	9	23	17.3	21	82	2
Recycling	$R_n = 85\%$	14	4	50	6.2	11	56	5
Pump inner	$A_n = 85\%$	37	10	28	4.9	13	39	6
Pump outer	$A_n = 85\%$	68	23	20	3.4	15	24	9
Puff outer	$I_n=70\text{A/m}$	69	29	10	1.6	26	6	20
Pump & puff outer	$A_n = 85\%$ $I_n=40\text{A/m}$	67	13	19	3.9	18	21	8

Table 1. (160mm)

Figure Captions

Fig. 1. The computational domain: SOL (white), divertor legs (green), inner boundary and private flux (yellow), neutral pump (red), and neutral injector (blue).

Fig. 2. Target plate solutions: (a) symmetric case, (b) electric bias $\Delta\Phi_{\text{wall}}=95$ V, (c) inner/private flux and (d) outer/SOL pumping with $A_n=85\%$ on the wall near the left target plate; poloidal projections of J_{\parallel} (solid green) and J_{sat} (dashed green) on right target; T_e (red) and n_i (blue) on left plate (solid) and right plate (dashed).

Fig. 3. Plasma parameters as functions of (a) electric bias $\Delta\Phi_{\text{wall}}$ and (b) thermo-electric bias $\langle\Delta\Phi_{\text{thermo}}\rangle$ for wall pumping (solid), private flux pumping ('o') and outer SOL pumping ('x'); $I_{\parallel}/I_{\text{sat, right}}$ (green), $\langle T_{e, \text{right}} \rangle / \langle T_{e, \text{left}} \rangle$ (red), $\langle n_{i, \text{left}} \rangle / \langle n_{i, \text{right}} \rangle$ (blue), and $\langle n_{n, \text{left}} \rangle / \langle n_{n, \text{right}} \rangle$ (purple). The black curves are (a) $\langle\Delta\Phi_{\text{thermo}}\rangle / 10\text{V}$, (b) $10 \times I_{\text{pump}} / I_{\text{sat, tot}}$.

Figures

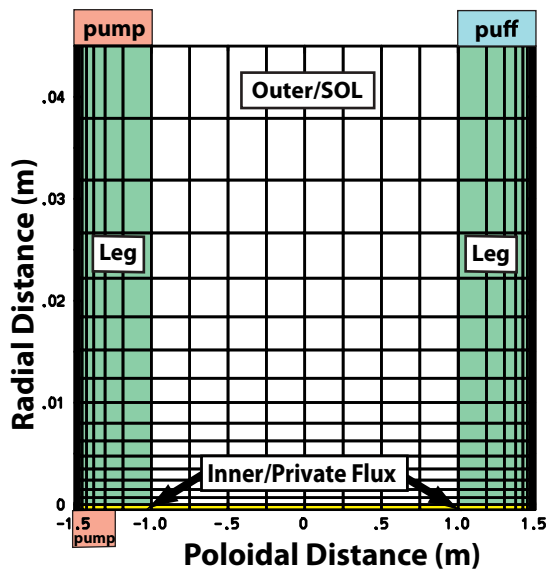


Figure 1. (75 mm)

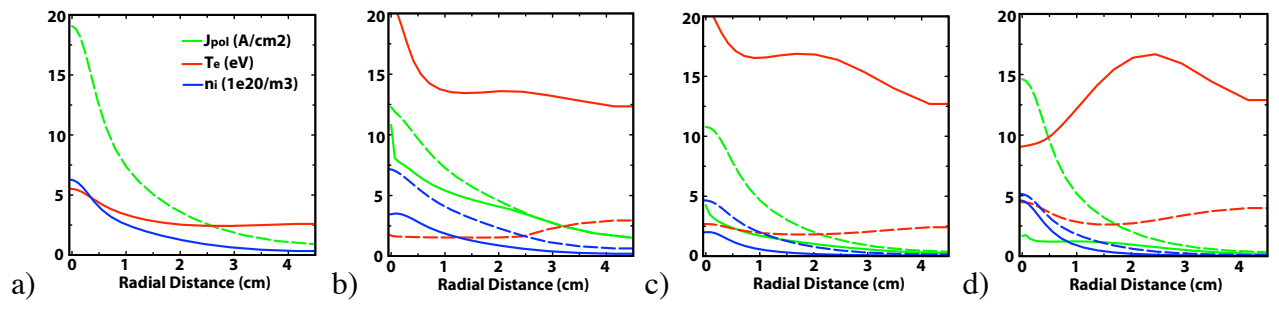


Fig. 2. (160 mm)

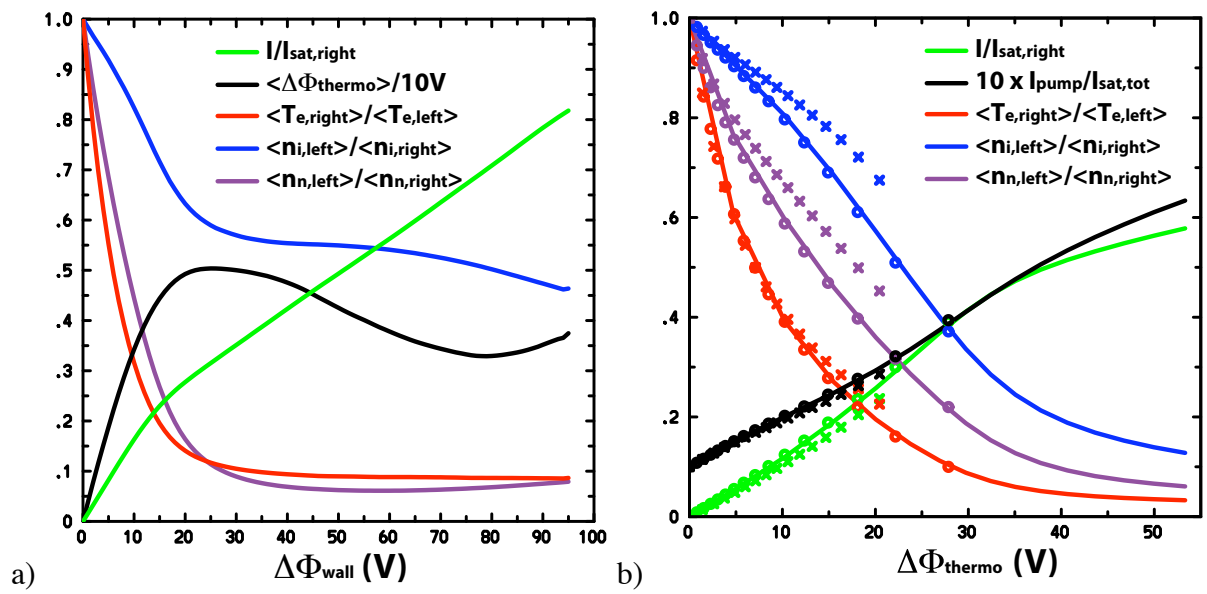


Figure 3. (160 mm)